Astron. Astrophys. 357, 1093–1104 (2000)

ASTRONOMY AND ASTROPHYSICS

Network and internetwork: a compared multiwavelength analysis

G. Cauzzi[1], **A. Falchi**[1], **and R. Falciani**[2]

[1] Osservatorio Astrofisico di Arcetri, 50125 Firenze, Italy
[2] Dipartimento di Astronomia e Scienza dello Spazio, 50125 Firenze, Italy

Received 24 December 1999 / Accepted 16 March 2000

Abstract. We analyze the temporal behavior of Network Bright Points (NBPs) using a set of data acquired during coordinated observations between ground-based observatories (mainly at the NSO/Sacramento Peak) and the Michelson Doppler Interferometer onboard SOHO.

We find that, at any time during the observational sequence, all the NBPs visible in the NaD_2 images are co-spatial within $1''$ with locations of enhanced magnetic field. The "excess" of NaD_2 intensity in NBPs, i.e. the emission over the average value of quiet regions, is directly related to the magnetic flux density. This property implies that, in analogy with the Ca II K line, the NaD_2 line center emission can be used as a proxy for magnetic structures.

We also compare the oscillation properties of NBPs and internetwork areas. At photospheric levels no differences between the two structures are found in power spectra, but analysis of phase and coherence spectra suggests the presence of downward propagating waves in the internetwork. At chromospheric levels some differences are evident in the power spectrum between NBPs and internetwork. At levels contributing to the NaD_2 emission the NBPs show a strongly reduced amplitude of oscillations at the p - mode frequencies. At levels contributing to the Hα core emission, the amplitude of network oscillations is higher than the internetwork ones. The power spectrum of NBPs at this wavelength shows an important peak at 2.2 mHz (7 minutes), not present in the internetwork areas. Its coherence spectrum with Hα wings shows very low coherence at this frequency, implying that the oscillations at these chromospheric levels are not directly coupled with those present in lower layers.

Key words: Sun: photosphere – Sun: chromosphere – Sun: magnetic fields – Sun: oscillations

1. Introduction

The chromospheric bright network has long been observed in narrowband spectroheliograms taken in the H and K cores of the Ca II resonance lines. The Ca II network typically shows H and K profiles with high double peaks and enhanced line wings that persist for extended periods of time (longer than 10 minutes, see, e.g., Rutten & Uitenbroek 1991). The chromospheric network emission pattern is cospatial with small-scale magnetic field concentrations, and defines the supergranular network boundaries. It is this atmospheric component that produces the correlation between H and K excess line-core flux and magnetic activity of cool stars (Schrijver et al. 1989).

The dynamics of the network elements, compared with the internetwork or quiet chromosphere, has been extensively studied (especially from the observational point of view) since these small-scale structures can be important in channeling the energy from photospheric layers to the transition region and corona (Kneer & von Uexküll 1986, 1993; Deubner & Fleck 1990; Kulaczewski 1992; Al et al. 1998).

An assessment of the spectral characteristic properties of Network Bright Points (NBPs) at different layers in the atmosphere has been provided by Lites et al. (1993) using spectral observations in the range of the Ca II H line. In their work, these authors analyzed spectrographic observations of a single network bright patch and of several internetwork points. The wavelength shifts of photospheric and chromospheric lines allowed them to perform a compared analysis between the dynamics of the two atmospheric components. One of the relevant characteristics they describe is that at chromospheric levels (Ca II H_3) the NBPs show long period oscillations ($\nu < 3$ mHz) not correlated with oscillations in the lower atmosphere, while they lack power at higher temporal frequencies. The internetwork regions display instead enhanced power at higher frequencies, well correlated with photospheric oscillations. The presence of these low frequency oscillations in the network has been confirmed by Lites (1994) also for the chromospheric He I 10830 line, in contrast to Bocchialini et al. (1994) which observe, for the same line, oscillations only in the 5 minutes range.

An enhanced power in the low frequency range for network points with respect to the internetwork has also been observed by Kneer & von Uexküll (1986) in the center of the chromospheric Hα line. These authors however interpret this feature as not due to oscillations, but of mainly stochastic origin, and attribute it to erratic motions of the corresponding photospheric footpoints.

The problem is still open, and further observations to better address this issue are required (Lites 1994). In particular one would need observations: 1- on a larger number of NBPs, to

Send offprint requests to: A. Falchi (falchi@arcetri.astro.it)

Table 1. Summary of the observations

Instrument	FOV	Spat. resol.	Observing λ (Å)	FWHM (Å)	Δt (s)
UBF	$2' \times 2'$	$0.5'' \times 0.5''$	5889.9 (NaD_2)	0.2	12
			6562.8 (Hα)	0.25	
			6561.3 (H$\alpha - 1.5$ Å)	0.25	
Zeiss	$2' \times 2'$	$0.5'' \times 0.5''$	6564.3 (H$\alpha + 1.5$ Å)	0.25	3
White Light	$2' \times 2'$	$0.5'' \times 0.5''$	5500	100	3
HSG	$0.75'' \times 2'$	$0.75'' \times 0.36''$	3904−3941 (CaII K)	0.035	
MDI	$10' \times 6'$	$0.6'' \times 0.6''$	6768 (Ni I)	0.1	60

improve on the statistics; 2- at different heights in the atmosphere, since the analysis of the coherence between fluctuations at different levels can help exploring the nature of oscillations. To this end, a reliable method for the identification of the same physical structure at different atmospheric levels is mandatory, since the inclination of the magnetic field could displace the chromospheric network points with respect to the corresponding photospheric ones.

In this paper, we address some of these issues, and present observational results on the NBPs and internetwork characteristics as derived from a multiwavelength analysis. The observations were obtained in August 1996, during a coordinated observing program between ground-based observatories and the Solar and Heliospheric Observatory (SOHO). For the ground-based observations we used the cluster of instruments at the NSO/Sacramento Peak R.B. Dunn Solar Telescope (NSO/SP-DST), that could provide a complete coverage at lower atmospheric levels. The dataset used is described in Sect. 2. General properties of a sample of NBPs, followed from the photosphere up to the chromosphere and including their relationship with the magnetic structures, are given in Sect. 3. The temporal development of the NBPs is described in Sect. 4. Sections 5 and 6 provide an analysis of the power, phase difference and coherence spectra for the fluctuations observed separately within the NBPs and the surrounding internetwork. Finally, discussion and conclusions are given in Sect. 7.

2. Observations and data reduction

A description of the general data acquisition has been presented in Cauzzi et al. (1997, 1999). Table 1 gives a summary of the observing setup, and we recall here only some short information on the data used in this paper. Monochromatic intensity images were obtained with the tunable Universal Birefringent Filter (UBF) and the Zeiss filter, at high spatial and temporal resolution. Several spectra were obtained around the chromospheric CaII K line with the Horizontal Spectrograph (HSG). The spectra have been acquired setting the spectrograph slit on different bright points at different times; the field of view in the HSG row of Table 1 hence refers to a single slit exposure. Onboard SOHO, the Michelson Doppler Imager (MDI, Scherrer et al. 1995) acquired data in high resolution mode, i.e. with an image scale of 0.605″/pixel. Maps of pseudo-continuum intensity, line-of-sight velocity, and longitudinal magnetic flux were obtained in the NiI 6768 Å line at a rate of one per minute for several hours. The line-of-sight velocity images were available in a binned 2x2 format, i.e. with an effective spatial scale of 1.2″/pixel.

We observed the small Active Region (AR) NOAA 7984 over 5 consecutive days (Aug. 15–19, 1996). Its activity was very low and although some stronger magnetic structures (a small spot and some pores) were present in the field of view (FOV), no major eruptions of magnetic flux were recorded. The situation was then appropriate to study and characterize the properties of NBPs visible within and around the AR. We remark that our set of data allows us to directly compare the NBPs as visible at different wavelengths with the corresponding magnetic field structure, and to follow them from the deep photosphere to the higher chromosphere. In this paper we analyze the data obtained on August 15th, 1996, since for that day we had the best uniformity in time coverage for NSO and MDI data. Fig. 1 shows the FOV at several wavelengths. The period of best seeing for ground-based observations ran from 15:15 to 16:05 UT. This interval is adequate for the study of network points, since it allows an analysis of their (possible) periodical properties, while they still maintain their identity (Lites et al. 1993; von Uexküll & Kneer 1995). MDI data were available for many hours around this interval; we consider in this work the period 14:00–17:00 UT.

The data were re-scaled to the 0.605″/pixel of the MDI maps, and the co-alignment of the whole dataset was obtained comparing the position of the prominent solar features, i.e. the little spot and pores (see Fig. 1). At each given time the alignment among the images acquired with different instruments was better than about 1″, the mean spatial resolution limit of the ground-based frames.

3. Characteristics of NBPs

In order to identify suitable network points, we first selected on the spectra bright features showing strong K_2 peaks and enhanced wings emission in CaII K. Since the NBPs lifetime is typically longer than 10 minutes (Rutten & Uitenbroek 1991), we further required that the points be visible for the entire observing period in the NaD_2 images as bright structures with intensity above the average. A total of 11 NBPs with the required characteristics were selected. They are distributed over the FOV both near the center of the AR and away from it, as can be seen in Fig. 1a. Several more network points (or structures) are visible on the longitudinal magnetic flux maps, but in this

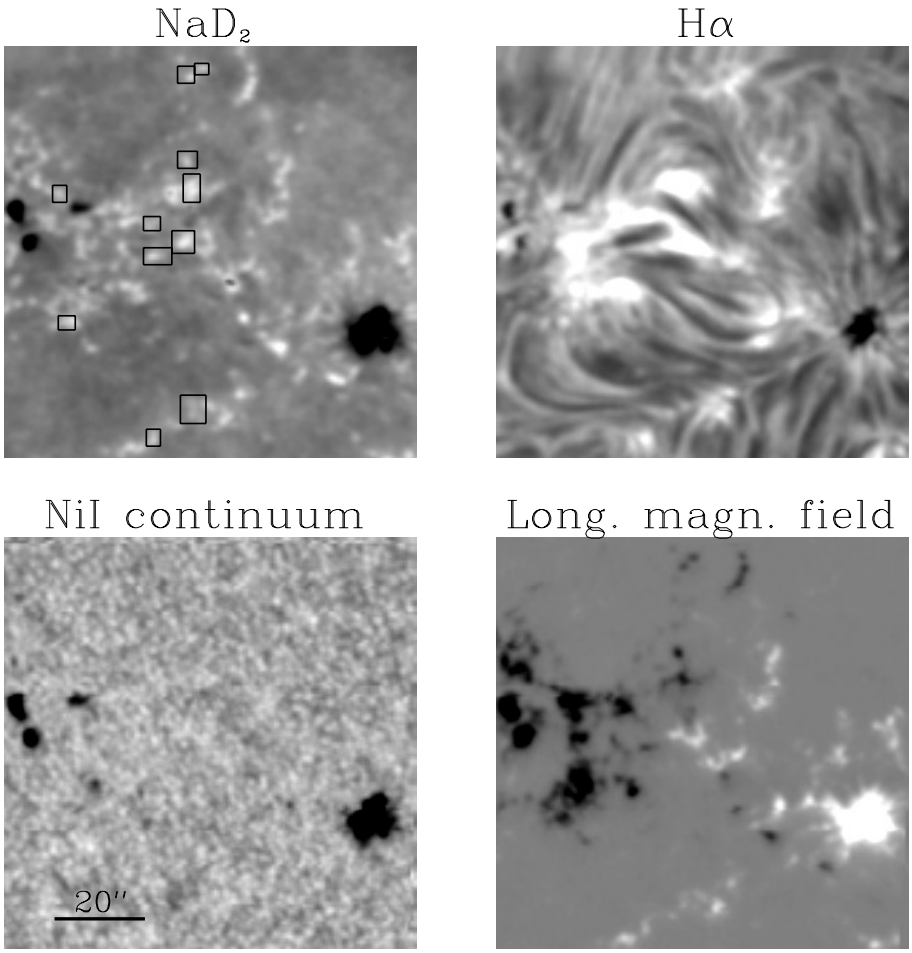

Fig. 1a–d. AR NOAA 7984 observed on Aug. 15, 1996, N29E16. a) NaD_2 image averaged over the time interval 15:15–16:05 UT. The black squares indicate the position of the NBPs analyzed in this work. **b**, **c** and **d** Same FOV as **a**, observed in Hα, NiI pseudo-continuum and longitudinal magnetic flux

work we limit our analysis to only these 11 points for which corresponding CaII K spectra are available.

3.1. Intensity and velocity

Within the areas enclosing the NBPs defined above, we tried to identify the bright points at each wavelength by choosing an intensity (or other signature) threshold that could clearly separate them from their surroundings.

On white light and NiI pseudo-continuum images, an intensity threshold cannot clearly discriminate between NBPs and other areas. The contrast averaged over the spatial locations corresponding to the NBPs is of the order of 1%, i.e. smaller than the rms noise calculated in quiet areas (about 3.5% and 2% for the white light and pseudo-continuum images, respectively). This is consistent with the observations of Topka et al. (1997), that find low continuum intensity contrast in network points with magnetic flux density smaller than ≈ 300 G (as typical of our points, see Sect. 3.2).

The line of sight velocities averaged over the NBP areas are small, about $80\,\mathrm{m\,s^{-1}}$ downward with respect to the average values over the quiet areas of the FOV. Since the standard deviation of the measurements is about $200\,\mathrm{m\,s^{-1}}$, for both NPBs and quiet areas, it is not possible to define a velocity threshold that allows to discriminate the NBPs within the FOV. The small average red-shift is however in agreement with recent observations by Solanki (1993) and Martínez-Pillet et al. (1994).

The NBPs are instead well visible in the images acquired in the Hα far wings and NaD_2 center, as sharp and isolated bright structures of comparable size ($3''-4''$wide). The bright points, as seen at these wavelengths, spatially coincide within the overlapping error of $1''$. In the Hα center images the morphology is less clear. The presence of contiguous features, at times brighter than the selected NBPs, made more uncertain their identification. In total, however, 10 of the 11 considered NBPs were unambiguosly identified in the Hα center images.

The characteristics of the NBPs for different signatures, including their typical contrast with respect to quiet areas, are summarized in Table 2. It must be remarked that the formation height of these signatures has been computed in a mean quiet atmosphere, i.e. that it represents only a *generic* indication for magnetic structures such as the NBPs. In particular, due to the Wilson depression, the radiation coming from photospheric magnetic structures is believed to be formed in deeper geometric layers with respect to non-magnetic ones. Since the spatial resolution for our observations is not sufficient to resolve the (supposedly) elementary magnetic fluxtubes (with dimensions smaller than $0.3''$, as seen for example in G-band images), the

Table 2. Characteristics of the NBPs at different atmospheric heights. The first column gives the formation height for each wavelength, computed in the quiet Sun VALC model (Vernazza et al. 1981), taking into account the different widths of the filters. The second column gives the typical diameter of the structures when they are clearly visible. The third column gives the intensity contrast values, averaged over time. A range of values is reported when variations are large over the sample.

Observed features	height(km)	size($''$)	ΔI/I
White Light	0	–	0.01
Hα wings	100.	3	0.04
Pseudo-continuum (Ni I)	100–200.	–	0.01
NaD_2	600.	3–4	0.1
Hα center	1500.	4	0.1–0.2

signals we analyze are a non-linear combination of magnetic and non-magnetic ones.

3.2. Magnetic structures

The selected NBPs are clearly recognizable on the MDI magnetic maps as sharp and isolated structures, $3''-4''$ wide. Each one corresponds to a patch of definite polarity, with magnetic flux densities ranging from a minimum of 30 G, to a maximum of about 250 G (for comparison, the spot in the FOV has a maximum flux density of 1100 G). The error on a single pixel in each image is given at about 15 G (Schrijver et al. 1997). Since the network fields are mostly vertical (see, e.g., Lites et al. 1999), the flux measure is only slightly affected by the position of the FOV on the solar disk ($\cos\theta \sim 0.9$).

The magnetic evolution of the NBPs is quite varied. Some of the points maintain stable positions and flux values, while others experience a steady increase during the observing period. In one single case we see a weak magnetic structure appearing during the observing sequence, simultaneously with the appearance of a network bright point.

The spatial correspondence between the NaD_2 network points and the magnetic structures is very good, and will be analyzed in more detail in the next section. The same correspondence is noticeable also for the network points as seen in the Hα wings, although this is less evident than for NaD_2 due to their lower contrast.

3.3. Magnetic structure and NaD_2 emission

We checked the spatial correspondence between the network points as visible in NaD_2 and in magnetic maps. To this end we first removed from both signatures, by means of appropriate smoothing techniques, short term variations due to noise and oscillations (especially in the 5-minutes range). We then subtracted a threshold, chosen as the average quiet area value for the NaD_2 images, and as the nominal data noise (15 G) for the magnetic ones. Finally, within the 11 selected areas, a NBP was identified in both signatures as the locus of the pixels exceeding 50% of the local maximum. This allowed its clear separation from the surroundings.

We find that, at *any* given time, the NaD_2 network points are coincident in position, size and shape with the corresponding magnetic patches, within $1''$ (the overlapping error). Any change in the characteristics of the NaD_2 NBPs reflect almost perfectly those of the magnetic features, within the temporal resolution of the MDI data. This is well exemplified in Fig. 2, where we show NaD_2 contours overlaying magnetic flux maps of several NBPs at two different times. To our knowledge, this is the first time that such a correspondence is reported at high spatial *and* temporal resolution. A good agreement between the chromospheric network emission pattern and the locations of enhanced magnetic flux had been noted in earlier works (Skumanich et al. 1975; Schrijver et al. 1989; Nindos & Zirin 1998) but mostly for the CaII K emission, with lower spatial and temporal resolution. No temporal resolution was available in the observations of Beckers (1976) or in those of Daras-Papamargaritis & Koutchmy (1983), that established a correlation between magnetic structures and facular structures in the wings of the Mgb lines.

In analogy with the CaII H and K case, we could establish a *quantitative* relationship between the NaD_2 excess and the magnetic flux density for the network points. This property implies that also the emission in the center of the NaD_2 line can be used as a proxy for the magnetic field structures. For sake of simplicity, the details of the determination of this relationship are given in Appendix A.

4. Temporal development: light curves

To study the temporal development of the NBPs, we computed the light curves for the bright points at each wavelength or signature. The curves for each NBP were obtained by selecting an area that contained the bright point throughout the whole observing period (even if it moved spatially), and then averaging, for each time, over all the pixels whose intensity exceeded the threshold value described in Sect. 3.1. A threshold equal to the nominal data noise was used for the magnetic curves. As said in Sect. 3.1, the NBPs are not directly visible in some photospheric signatures, such as white light, NiI pseudo-continuum and velocity images, hence we couldn't use an intensity (velocity) threshold to obtain the corresponding light curves. To guarantee the comparability with the other light curves, in these cases we computed, at each time, the average value over the spatially corresponding *magnetic* areas.

We also computed the light curves of 11 areas randomly selected in the quiet regions of our FOV, and of size comparable to that of the NBPs (about $3''\times3''$). No threshold was applied for their computation. These quiet areas should represent the so-called internetwork regions, which appear field-free at MDI sensitivity. Using the same number of internetwork areas as of network bright points, and performing the analysis in the same way, will give us confidence in the comparison in a statistical sense. We remark that this is not always the case, especially for spectrographical observations where the slit samples a number of internetwork points that is usually much larger than that of network structures. In Fig. 3, as an example, we show the light curves of different signatures for a NBP. Fluctuations are evi-

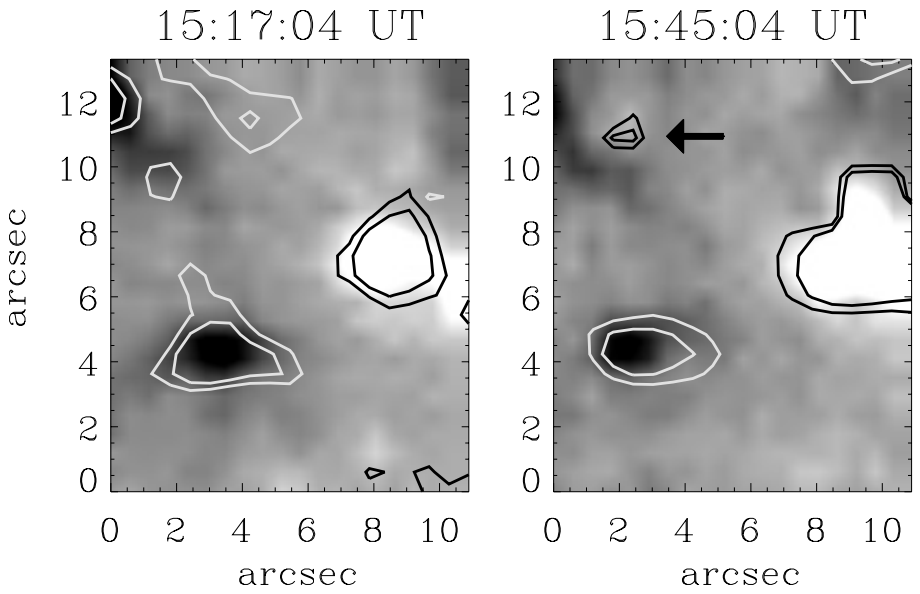

Fig. 2. Longitudinal magnetic flux maps (scaled between +100 and −200 G) for two different NBPs at two different times. The contours represent the NaD_2 threshold defining a network bright point. One can see the change in shape and position of the magnetic structures during this interval, and the corresponding changes in NaD_2 emission. The arrow indicates a new NBP appeared simultaneously with a weak magnetic structure

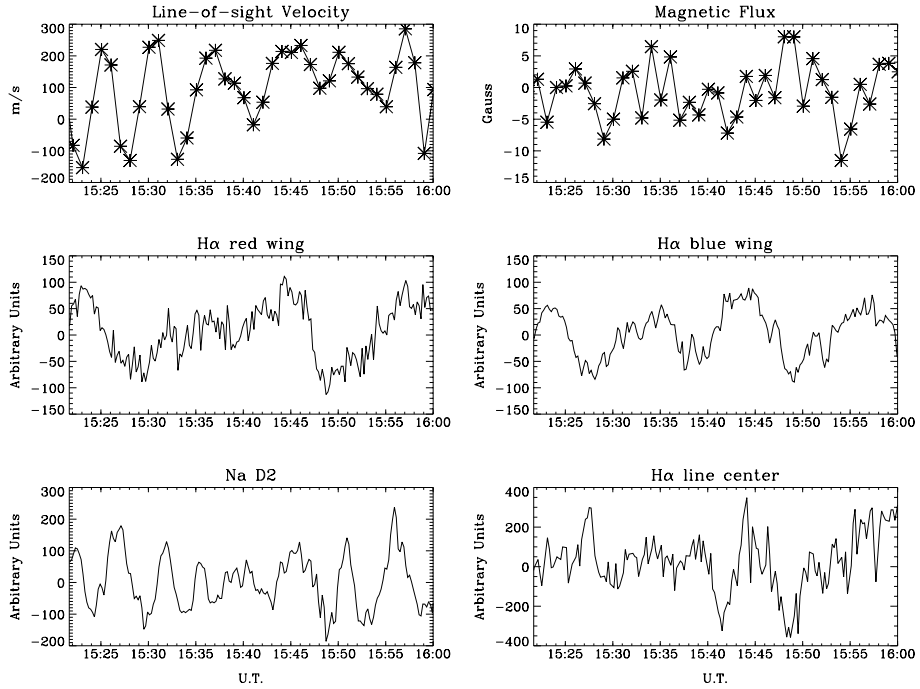

Fig. 3. Temporal evolution for a single NBP of velocity, magnetic flux density, intensity in Hα wings, NaD_2, Hα. Long-period trends have been subtracted using a smoothing window of 600 s (see next section). Intensity variations are after subtracting a value of 10^4 arbitrary units

dent at each wavelength. The red and blue wings of Hα show a very similar temporal evolution, with simultaneous intensity variations of the same magnitude for most NBPs. For other signatures a direct comparison does not show any simple relation between the variations at different atmospheric heights.

We must comment here on the fact that most authors, when studying the temporal properties of network points, use a different method to determine the "light curves". Basically, the network points are spatially identified using the temporal average of some suitable signature, and then the temporal development of each *image pixel* belonging to the average structures is considered and analyzed. We believe that the method we adopted has several advantages: - Since the network points might move over the course of time, they do not always correspond spatially to the structures identified on the average maps. Our method guarantees that the structure is properly followed in time, avoiding the loss of relevant pixels, or the inclusion of spurious ones; – If the magnetic structure giving rise to the network point inclines with height, a set of pixels identifying the NBP at a given wavelength might not well represent the same structure at a different wavelength. This is especially relevant when performing comparisons between different atmospheric layers, for example in the phase difference analysis of Sect. 6. We overcame this problem by selecting areas large enough to include the NBPs at each wavelength and each time, as explained earlier.

Computing the light curves as an average over a given area implies the assumption of a spatial coherence over the whole area (of about $3'' \times 3''$, equivalent to a spatial frequency of about 3 Mm^{-1}) competing to each NBP. This seems a reasonable assumption because we do not see any significant inhomogeneities within the single structures.

5. Power spectra

A search for possible periodicities in the fluctuations of the NBPs light curves was performed using temporal power spectra. Before computing the power spectra, the light curves were detrended using a smoothing window of 600 s. A check on this procedure showed that changing the smoothing window between 360 s and 840 s affected the power at frequencies lower than 1.2 mHz, but without changing the frequency of the peaks. The power at higher frequencies remained unaffected.

A power spectrum was computed for each light curve of the 11 NBPs and of the 11 internetwork areas. To analyze the differences between these two atmospheric components, we averaged separately the power spectra over all of the NBPs and over all of the quiet regions. In Fig. 4 we show some of these averaged curves. It must be remembered that the NSO and MDI observations have different temporal coverage (50 and 180 minutes, respectively) and temporal resolution (12 s and 60 s), so that lower temporal frequencies are better represented in the NiI series, while frequency coverage extends to higher frequencies for ground-based data. However, the power at $\nu \geq 8$ mHz in all the ground-based signatures is due essentially to noise (Fig. 4), hence the analysis can be limited to the frequency coverage of the NiI observations, 0–8 mHz.

We describe here the power spectra characteristics from lower photospheric signatures to higher chromospheric ones. Intensity fluctuations may be plausibly interpreted as temperature fluctuations for photospheric LTE signatures such as Ni I or the Hα wings, formed over depths where the velocity gradient is small. In these cases, the intensity fluctuations directly reflect fluctuations of the source function (the Planck function) and hence of temperature. In the center of chromospheric lines as NaD_2 or Hα the NLTE effects are important and the intensity fluctuations are the response to temperature, density and even velocity changes (Cram 1978) and then are a sort of average of the variation of the state variables of the chromosphere.

5.1. Photospheric signatures

In Fig. 4a,b,d we show the power spectra of Ni I pseudo-continuum intensity, Ni I velocity and Hα red wing intensity. The power spectra computed for white light intensity (not shown in figure) and for the NiI pseudo-continuum are very similar, and we are confident that we can compare the two series of observations, even if their frequency resolution is different. The Hα blue wing spectrum (not shown in figure) has a similar behaviour but a lower amplitude with respect to the red wing (see Table 3). A value smaller than 1 for the ratio of the power in the blue and red wings of Hα is consistent with the observations of Bertello (1987), that found the same trend for the power of velocity oscillations in the wings of photospheric lines formed at heights lower than 150 km.

As is well known, the distribution of power for the photospheric velocity fluctuations is rather different from the one of pseudo-continuum intensity fluctuations (Fig. 4a,b). The velocity power is concentrated around the range of frequencies corresponding to the 5-minutes oscillations. The pseudo-continuum power spectrum peaks at low frequencies, around 1.5 mHz and then show a decay that might indicate the stochastic character of the granulation intensity variation, as already reported for the first time in Noyes (1967).

As a global characteristic, power spectra computed in photospheric signatures do not show any significant difference between network and internetwork structures within the 50% confidence limit (Fig. 4a,b,d). This result is consistent with previous spectral observations by several authors (Deubner & Fleck 1990; Kulaczewski 1992; Lites et al. 1993) that analyzed both intensity and velocity oscillations in the photosphere for network and internetwork features.

The power spectrum of the magnetic flux variations averaged over the NBPs is shown in Fig. 4c. Internetwork areas are not considered because the noise in the magnetic flux measure is too high for a reliable determination of fluctuations. Significant peaks are visible at low frequency (around 1.5 mHz), indicating long term evolution of the magnetic field, and around 3.5 mHz corresponding to the 5 minutes oscillations. A signal at the latter timescale might represent the magnetic response to oscillations already present in the photosphere and be of importance in the context of generation and dissipation of MHD waves in the solar atmosphere (Ulrich 1996). Observations of flux variations in small magnetic structures are scarce in the literature, but we can compare this result with those presented by Norton et al. (1999), that used a similar set of MDI data obtained in the area of a big sunspot. They found a significant peak near 5 min only for structures whose magnetic flux density exceeded 600 G, while the points we analyzed had a maximum value of about 300 G.

5.2. Chromospheric signatures

The intensity power spectra computed in chromospheric signatures display strong differences between NBPs and internetwork as shown in Fig. 4e,f. We will analyze in detail these differences, keeping in mind that the regime of oscillations changes with height in the chromosphere.

First of all we notice that the power spectrum of internetwork intensity fluctuations in NaD_2 shares some characteristics with the photospheric NiI velocity power spectrum rather than with the one of Ni I intensity. In particular the strongest peak appears around 3.5 mHz, while the enhanced low frequency component, typical of photospheric intensity power spectra, is lacking. This characteristic could be explained if the intensity fluctuations in the NaD_2 line center were related more to velocity than to temperature perturbations. This might be indirectly confirmed by the results of Pallé et al. (1999) in their study of the current performances of the GOLF experiment on SOHO. In determining

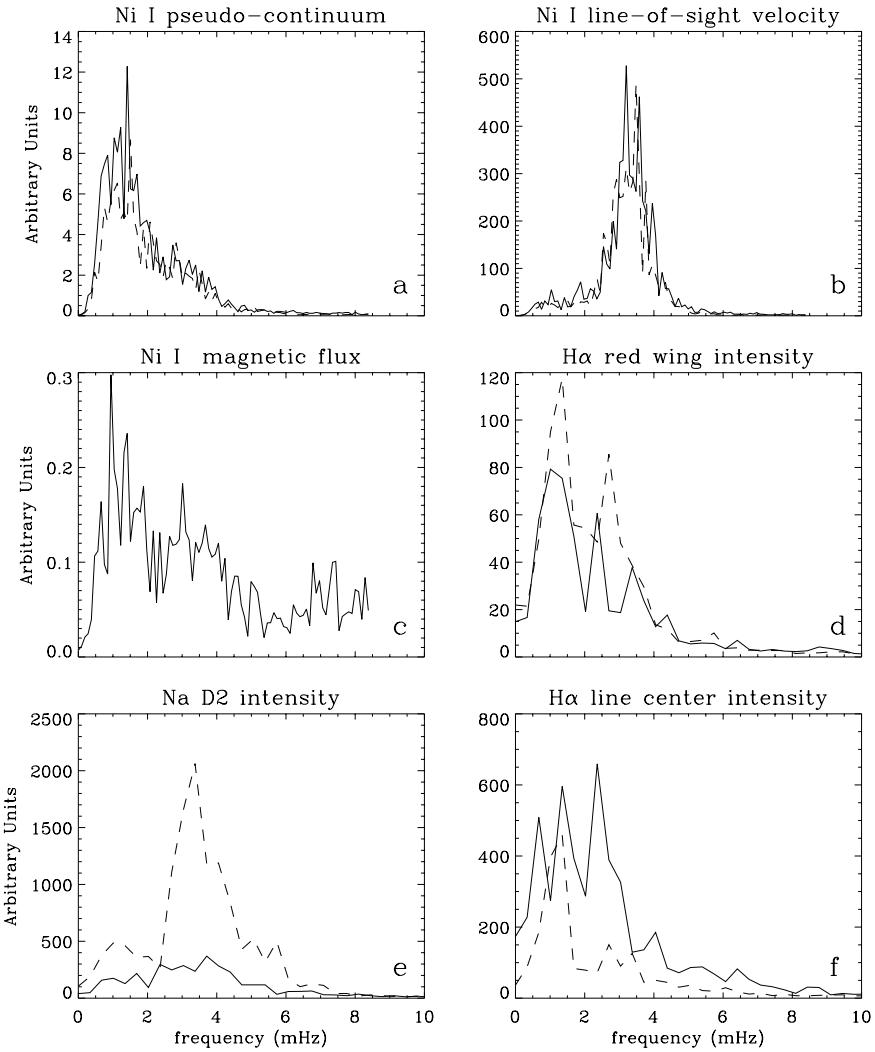

Fig. 4a–f. Power spectra in arbitrary units, averaged for NBPs (solid) and internetwork regions (dashed). The 50% confidence limit is given by the range $0.8-1.5\times$ the actual power values; for clarity error bars are not plotted in the figure

the relative contributions of velocity and intensity signals to the intensity variations measured in the blue wings (-100 mÅ) of the sodium doublet, they conclude that the effect due to "pure" intensity changes is only 14% that of velocity changes for the *p* - mode frequency range. Since the width of the filter used for our observations includes that same portion of the line wing, this conclusion might apply, at least partially, also to our case.

Comparing network and internetwork power spectra for NaD_2, we see that the power of the NBPs is smaller than the corresponding power for internetwork at each temporal frequency. In particular, even if both NBPs and internetwork points show a maximum around 3.5 mHz, the power at this frequency is almost an order of magnitude smaller in the NBPs. (Fig. 4d suggests that this effect might be already present in the wings of Hα, although its amplitude is not large enough to give an unambiguous result). This suppression of power in the NBPs indicates that the presence of the magnetic field in some way perturbs and reduces the oscillations at low chromospheric levels, especially in the p-mode range. A compression of power in magnetic structures at frequencies below 7–8 mHz, for lines formed at similar heights, has not been reported by other authors. Only Al et al. (1998) observe a similar effect, but much smaller, for the power spectrum of velocity fluctuations measured in the center of NaD_2 with a narrowband filter (30 mÅ). We think that the stronger effect seen in our observations is real because our analysis selects the horizontal scale typical of chromospheric network to determine the light curves and the power spectra (see Sect. 4), and is therefore more suitable to outline characteristics and differences on the same horizontal scale for NBPs and internetwork areas.

The power spectrum computed for the intensity of Hα center is shown in Fig. 4f. For both NBPs and internetwork the power distribution peaks at low frequencies ($\nu \leq 3$ mHz), without any relevant peak at the p-mode frequencies. No enhanced power for "3-minutes" oscillations ($\nu > 5$ mHz), is detectable in the internetwork. This is consistent with observations in the Hα center by Cram (1978) and in the Ca II - H3 by Lites et al. 1993 showing a power peak in the "3 minutes" range only for velocity power spectrum.

The spectrum of NBPs in Hα line has a power higher than that of the internetwork areas at each frequency, reversing the effect present in the NaD_2 line, and shows three well separated peaks reminiscent of the peaks observed by Lites et al. (1993).

Table 3. Power values in arbitrary units for various observed features. A range of values is reported when variations are large.

frequency range	1.5–2.5 mHz		3.0–4.0 mHz	
Observed features	NBP	Internet.	NBP	Internet.
Pseudo-continuum (Ni I)	8–2	8–2	2	2
Velocity (Ni I)	–	–	400	400
Magnetic Flux	0.15–0.1	–	0.13	–
Hα red wing	80–40	100–60	30	30
Hα blue wing	50–30	75–45	20	25
NaD_2	–	–	300	2000
Hα center	650	100	–	–

Table 4. Phase difference $\Delta\Phi$ in degrees and coherence **C** for the considered pairs

frequency range		1.5 - 2.5 mHz		3.0 - 4.0 mHz	
Observed pairs		NBP	Internet.	NBP	Internet.
Hα + 1.5 Å /Hα − 1.5 Å	$\Delta\Phi$	0	0	7	10
Hα + 1.5 Å /Hα − 1.5 Å	**C**	0.85	0.95	0.8	0.9
Hα + 1.5 Å / WL	$\Delta\Phi$	-8 - 0	10 - 5	0	0
Hα + 1.5 Å / WL	**C**	0.8	0.95	0.75	0.95
Magnetic flux / Velocity	$\Delta\Phi$	–	–	-20	–
Magnetic flux / Velocity	**C**	–	–	0.4	–
Hα center /Hα − 1.5 Å	$\Delta\Phi$	0	0	–	–
Hα center /Hα − 1.5 Å	**C**	0.45	0.72	–	–
Hα center /Hα + 1.5 Å	$\Delta\Phi$	0	0	–	–
Hα center /Hα + 1.5 Å	**C**	0.5	0.65	–	–

The more relevant peak is around 2.2 mHz ("7-minutes" oscillations) and is lowered about a factor 6 in the internetwork. We cannot judge on the relevance of the peak around 1.3 mHz, since its amplitude is heavily affected by the smoothing window, as described in Sect. 5, and we cannot consider real the peak at 0.6 mHz, because it is related to the time interval of our observations. However, the increasing power at low frequencies in the spectrum of NBPs suggests that the rôle of the magnetic field in the oscillations, detectable at high chromospheric levels, is certainly different from the one at lower levels and strenghtens the hypothesis of magnetic-hydrodynamic waves present at these high levels.

Characteristics of power spectra for network and internetwork are summarized in Table 3 for the two relevant frequency windows 1.5–2.5 mHz and 3–4 mHz.

6. Phase difference and coherence spectra

In order to look for propagation characteristics of waves at different heights in the atmosphere, we computed phase difference ($\Delta\Phi$) and phase coherence (C) spectra for many signature pairs (Straus 1995). We exclude in this analysis the NaD_2 signature because, if the measured intensity oscillations are due essentially to velocity oscillations, we cannot establish the direction of the motion and hence assign the correct value to the phase difference.

Following Edmonds & Webb (1972), we adopted a smoothing width of about 1.5 mHz in the Fourier domain for the computation of phase and coherence spectra. Frequencies smaller than 0.7 mHz hence do not convey any significant information. Taking into account our smoothing width, a coherence smaller than $\sim$0.5 implies that phase differences at those frequencies are completely unreliable.

NSO and MDI data were analyzed independently, using their own frequency resolution and coverage. Finally, the study was performed separately for internetwork and network areas, to distinguish between features with different magnetic characteristics. We describe the characteristics of the spectra from lower photospheric layers through higher chromospheric ones.

In Fig. 5 left and central column, we show intensity (I−I) phase difference and coherence spectra for the pairs Hα + 1.5 Å/Hα − 1.5 Å, and Hα + 1.5 Å / white light, originating at photospheric levels. We use here the white light signal (and not the NiI pseudo-continuum) in order to keep the maximum possible frequency resolution. Phase difference and coherence spectra between magnetic flux density and velocity (B−V) for the NBPs are shown in Fig. 5 right column.

To search for the relationship between the oscillations present at chromospheric and photospheric levels we computed the I−I phase difference and coherence spectra separately for the pairs Hα center / Hα −1.5 Å and Hα center / Hα +1.5 Å, shown in Fig. 6. At each considered atmospheric level, a general characteristic is that the coherence for NBPs is smaller than for internetwork, hence the phase values for NBPs are more uncertain.

We examine different signature pairs separately in the two frequeny intervals 1.5–2.5 mHz and 3–4 mHz, disregarding the features with negligible power, and we summarize in Table 4 the phase and coherence values for each pair.

6.1. Low frequency (1.5–2.5 mHz)

For both internetwork and network points the I−I phase difference between the Hα red and blue wings is 0°. The two signals should be in phase if the observed oscillations are due only to temperature and in antiphase if due to velocity. We can then state that the observed oscillations at low frequencies are essentially due to temperature oscillations.

It follows from the previous considerations that the analysis of the phase difference spectra between the Hα red wing and white light is essentially a study of the correlation between temperature oscillations at slightly different levels ($\Delta h \leq 100$ km in the quiet average photosphere). For internetwork areas the extremely high coherence makes the $\Delta\Phi$ value (5–10°) highly significant (see Table 4) and strongly suggests that the observed power is due to oscillations. A positive value of $\Delta\Phi$ between two layers with decreasing heights, indicates the presence of waves directed radially inward. For the internetwork areas, free from magnetic fields, at the spatial frequency of about 3Mm^{-1} used

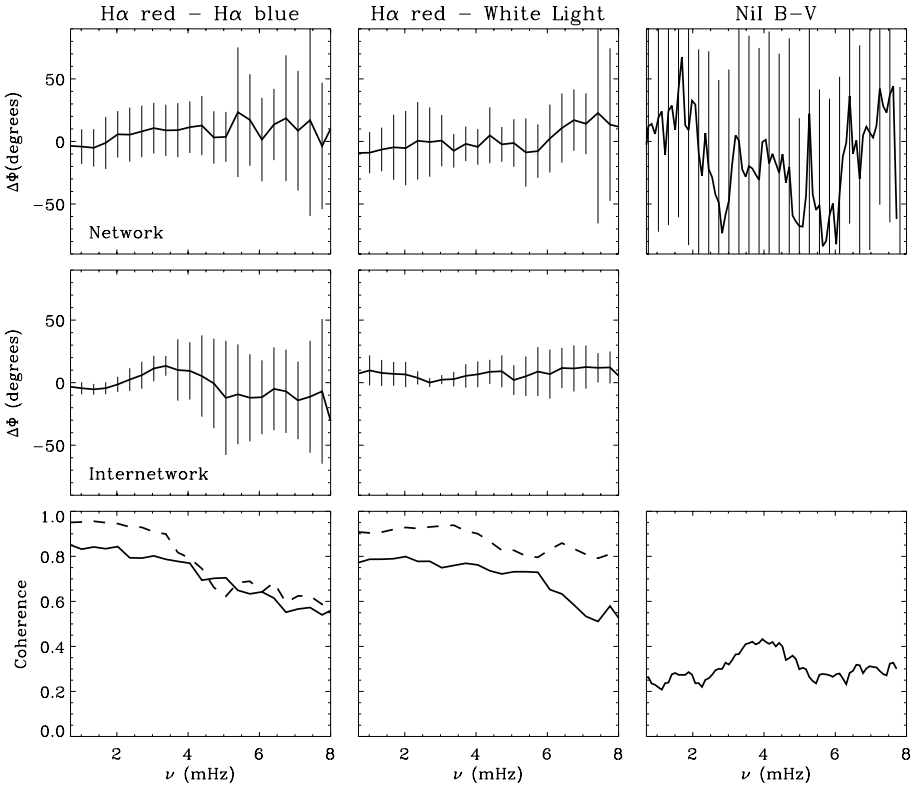

Fig. 5. Top and mid panels show the phase difference I − I, as a function of frequency, of photospheric signatures averaged for network and internetwork regions. Vertical bars, representing 1σ error associated with the mean phase value, are clipped if higher than the y-axis limits. The bottom panels show the phase coherence spectra (computed with a smoothing width of 1.5 mHz, see text) averaged for network (solid line) and internetwork (dashed line) regions

in our analysis and within the considered frequency range, these waves might be interpreted as gravity waves (Straus 1995). This same interpretation has been adopted for internetwork by Rutten (2000), who reported a similar value of $\Delta\Phi$ between the intensity of two continuum levels observed by TRACE. Downward directed gravity waves had been proposed earlier by Staiger et al. (1984) to explain similar phase differences for velocity signatures at photospheric levels.

At chromospheric levels, the most significant peak in the power spectrum of the Hα center intensity appears at 2.2 mHz for NBPs and is not related to the oscillations present at photospheric levels (**C** $= 0.45$ between Hα center /Hα $+1.5$ Å, see Table 4). This means that at chromospheric levels the NBPs experience a new regime of oscillations that seem to be independent from what happens in photosphere.

6.2. p-mode frequency (3.0–4.0 mHz)

In the p-mode range of frequencies, for internetwork there is a 10° phase lag between the two Hα wings (see Table 4) that can be due to different coupling of velocity and intensity fluctuations in the two wings. This effect has been extensively studied for photospheric lines by Cavallini et al. (1987) and Alamanni et al. (1990).

As described in Sect. 5.1, the presence of a peak at these frequencies spectra could betray the presence of MHD waves in the network structures. In the limit of ideal MHD, a definite phase relation between velocity and magnetic field variations is expected as signature of Alfvèn waves ($\Delta\Phi = 0^\circ$) or magnetoacoustic waves ($\Delta\Phi = 90^\circ$, with v leading B. See Ulrich 1996). However, we find a very low coherence (< 0.4) at all frequencies in the NBPs, i.e. the magnetic fluctuations are not related to the velocity ones, at least with the present sensitivity and resolution.

7. Discussion and conclusions

The observations presented in this paper allowed us to define the characteristics of network bright points at different atmospheric heights, and to compare them with those of the surrounding internetwork areas. We improved on the existing statistics using a good-sized sample of NBPs, and the same number of "test" internetwork areas, defined in a comparable way. The method we adopted to study the temporal evolution of NBPs insures that each bright structure is properly followed in time and position at each height. In fact, the evaluation of the light curves and their properties after a spatial averaging over a well defined area guarantees that we are studying the same NBP at all heights, and avoids the problem (first pointed out by Lites 1994) of a possible structure displacement due to the magnetic field inclination. Given the characteristic horizontal size of the NBPs, the analysis and the comparison of power spectra and phase differences concern the propagation of waves pertaining to a horizontal wavenumber of about 3 Mm^{-1}.

The quasi-simultaneous series of NaD_2 images and of MDI maps allowed us to establish for the first time a correspondence between NaD_2 bright network and magnetic network at high spatial and temporal resolution. A correspondence between bright chromospheric structures (Ca II, Lyα, Mg I and UV continuum) and magnetic structures had been observed before, but

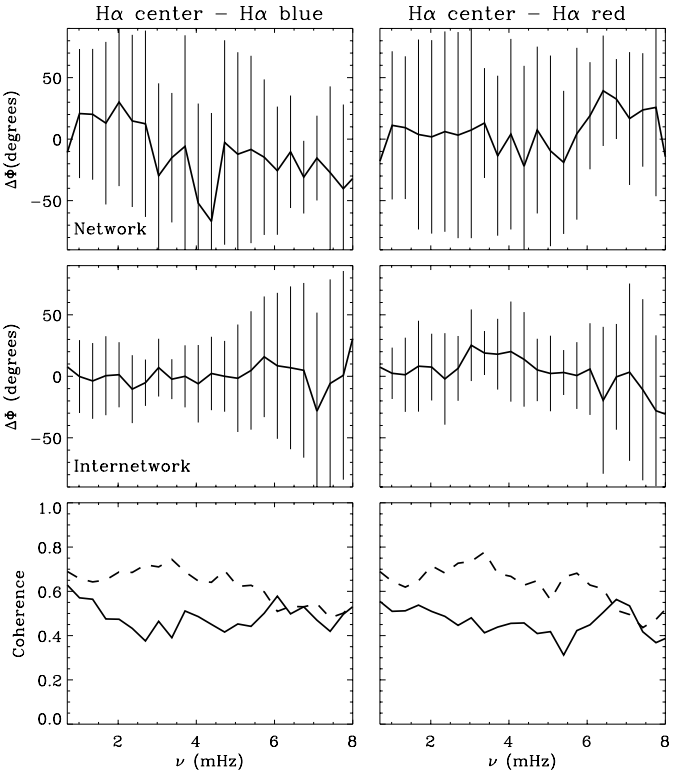

Fig. 6. Top and mid panels show the phase difference I − I, as a function of frequency, for the pairs Hα center / Hα -1.5 Å and Hα center / Hα $+1.5$ Å averaged for network and internetwork regions. Vertical bars, representing 1σ error associated with the mean phase value, are clipped when higher than the y-axis limits. The bottom panels show phase coherence spectra (computed with a smoothing width of 1.5 mHz, see text) averaged for network (solid line) and internetwork (dashed line) regions

not at this high temporal resolution. We also established for the NBPs a quantitative relationship between the Na excess and the corresponding absolute value of magnetic flux density. This relationship is best expressed by a power law with an exponent very close to the one found by Schrijver et al. (1989, 1996) for the Ca II - K excess, and indicates that the emission in NaD_2 may be used as a proxy for the magnetic flux density.

The NBPs considered in this work have the following properties: - are bright in the Ca II wings and in the Ca II K_2 peaks; - are visible in the NaD_2 images for about 1 hr; - coincide spatially with the magnetic structures; - are nearby or within a lower activity region. The general characteristics found for these NBPs do not differ from the ones derived in absolutely quiet regions (Deubner & Fleck 1990, Lites et al. 1993).

Our results referring to photospheric and chromospheric properties are so summarized:

At photospheric levels: No difference is detected between network and internetwork power spectra, either in intensity or in velocity, within the limits of sensitivity and accuracy of the instruments used for this work. The phase difference spectra between photospheric signatures in general do not show different characteristics for network or internetwork. However, when analyzing the phase difference between Hα red wing and white light images($\Delta h \leq 100$ km), we find $5^\circ \leq \Delta\Phi \leq 10^\circ$ in the frequency window 1.5–2.5 mHz and in the internetwork. (The $\Delta\Phi$ value is more uncertain in the network, due to a lower coherence value). A phase lag of this amplitude and sign is usually considered a signature of gravity waves directed radially inward. A possible explanation for their origin might be sought in recent models of convection, described as a non-local process driven by *cooling* at the solar surface rather than by heating from the lower layers (Spruit, 1997). One can imagine that the downward flowing cooled plasma can trigger some inward directed waves, and hence justify the fact that the external layers "lead" the deeper layers. The general inhibition of convection in magnetic structures might be the reason for the lack of this signature in network points.

The power spectrum of the magnetic flux variations in NBPs shows a small but significant peak around 3 mHz, that could be related to a "transformation" of acoustic waves into MHD waves. However, the phase difference and coherence spectra between magnetic flux and velocity (B−V) for the NBPs indicate a very low correlation between the two signals so we cannot conclude anything on the presence of MHD waves within the network points.

At chromospheric levels: Network and internetwork areas have a rather different behaviour in the power spectra. We do not see any evidence for the typical chromospheric period of 3 minutes (but it must be reminded that they are best seen in velocity variations rather than intensity). In the low chromospheric levels, where NaD_2 originates, the NBPs power spectrum is compressed at all frequencies if compared to the internetwork, while in the high chromosphere, where Hα originates, the power of NBPs is higher than the one of internetwork. This opposite effect may be an indication that the magnetic field disturbs and reduces the amplitude of oscillations already present in the low chromosphere while it assumes a leading rôle in the high chromosphere.

In the layers contributing to the NaD_2 emission it seems that the oscillations present in network points change regime with respect to both the photosphere and the high chromosphere and we think that it would be important to perform observations of NBPs in tha Na line, with high spectral resolution. Unfortunately we cannot analyze the phase difference spectrum for NaD_2 intensity fluctuations with respect to others formed at different layers, since the NaD_2 intensity fluctuations, measured with the UBF filter (FWHM$= 0.2$ Å), are more related to velocity than to temperature fluctuations (see Sect. 5.2).

The power spectrum of Hα intensity in NBPs has the more relevant peak at 2.2 mHz, but this signal is not correlated with the photospheric fluctuations, as indicated by the very low coherence measured at all frequencies between the Hα core and the blue and red wings. We can then confirm, using a larger sample of NBPs, the presence of the peak found by Lites et al. (1993) around 2 mHz in the power spectrum of K3 velocity fluctuations for one network point. Kalkofen (1997) and Hasan & Kalkofen (1999) proposed an explanation for this peak in terms of transverse magneto-acoustic waves in magnetic flux tubes,

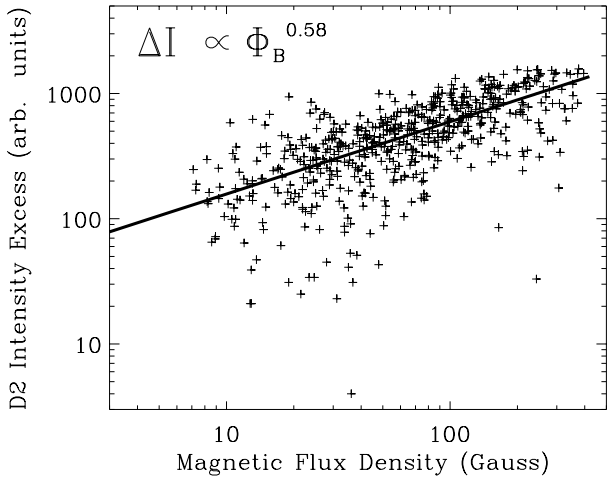

Fig. A1. Scatter diagram of the NaD_2 intensity, after subtraction of a threshold of about 10^4 (see text), vs. the absolute longitudinal magnetic flux density. All the 11 analyzed NBPs are plotted. Solid line is the power law fitting described in the text

excited by granular buffeting in the solar photosphere. In their model the low coherence between photospheric and chromospheric signatures could be explained by a partial conversion of the transverse waves to longitudinal modes in the higher chromosphere.

A general result of our analysis, valid from the low photosphere to the high chromosphere, is that the NBPs always show a coherence lower than the internetwork, pointing out that the presence of the magnetic field changes the propagation regime of waves with respect to the non-magnetic regions.

Acknowledgements. The authors are indebted to the NSO/SP-DST staff for the generous telescope time allocation and the unvaluable help during the observations. The authors express their thanks to the MDI team (P.I. P.H. Scherrer) for the efficient support during the observing run and their dedication in operating this instrument. MDI is part of SOHO, the Solar and Heliospheric Observatory, mission of international cooperation between ESA and NASA. We woud like to thank Thomas Straus for his comments during the preparation of this paper and for fruitful discussion on the phase difference problem.

Appendix A: a relationship between Na excess and magnetic field

A quantitative relationship between the CaII K line core intensity and the absolute value of the magnetic flux density has been clearly established by several studies (Skumanich et al. 1975; Schrijver et al. 1989; Nindos & Zirin 1998). The best agreement with the data is given by a power law relation with an exponent of 0.6 (Schrijver et al. 1989). Given the excellent spatial coincidence of the sodium network points and the magnetic structures present in our data (see Sect. 3.3, we searched for such a quantitative relationship also for this case.

Fig. A1 shows a scatterplot of the sodium "excess" for the 11 NBPs, vs. the corresponding absolute values of magnetic flux density. As done by Schrijver et al. (1989, 1996) for the CaII K emission, we subtracted to the NaD_2 intensities a threshold equal to the average intensity in the quiet areas (10^4 in arbitrary units). The graph was obtained plotting the temporal average of both the sodium intensity and magnetic flux. It does not display, hence, any temporal variation of either quantity, but only a general trend among the persistent structures. Five-minutes oscillations do not play a role in this relationship, nor do they contribute to the scatter of the points. Saturation, as reported by Schrijver et al. (1989) is not apparent in our data, but it must be remarked that the maximum value of the magnetic flux density for the average quantities is below 400 G, the "critical" value indicated by those authors.

The sodium excess is best fitted by a power law of the type $\Delta I \propto \Phi^{\beta}$, with β=0.58 $\pm$0.1. The exponent is very close to β=0.6$\pm$0.1 found by Schrijver et al. (1989, 1996) for the CaII K excess. These results indicate that the emission in the center of the NaD_2 line is also a good proxy for the magnetic flux density and, at least for values of magnetic flux density smaller than a few hundred G, its use is equivalent to that of the CaII K emission.

References

Al N., Bendlin C., Kneer F., 1998, A&A 336, 743
Alamanni N., Bertello L., Righini A. et al. 1990, A&A 231, 518
Beckers J. M., 1976, Air Force Geophysics Laboratory Report, 76-0131
Bertello L. 1987, Ph. D. Thesis, University of Firenze, Italy
Bocchialini K., Vial J.C., Koutchmy S., 1994, Ap. J. 423, L67
Cavallini F., Ceppateli G., Righini A., Alamanni N. 1987, A&A 173, 161
Cauzzi G., Vial J.C., Falciani R., Falchi A., 1997, ASP Conf. Ser. Vol. 118, Schmieder B., del Toro Iniesta J.C., Vázquez M. (eds.), p. 309
Cauzzi G., Falciani R., Falchi A., Vial J.C., 1999, ESA SP-448 Conf. Ser., ed. A. Wilson, in press
Cram L.E., 1978, A&A 70, 345
Daras-Papamargaritis H., Koutchmy S., 1983, A&A 125, 280
Deubner F.L., Fleck B., 1990, A&A 228, 506
Edmonds F.N., jr., Webb C.J., 1972, Solar Phys. 22, 276
Hasan S.S., Kalkofen W., 1999, ApJ 519, 899
Kalkofen W., 1997, ApJ 468, L69
Kneer F., von Uexküll M., 1986, A&A 155, 178
Kneer F., von Uexküll M., 1993, A&A 274, 584
Kulaczewski J., 1992, A&A 261, 602
Lites B.W., 1994 In: Carlsson M. (ed.), Chromospheric Dynamics, p. 1
Lites B.W., Rutten R.J., Kalkofen W., 1993, ApJ 414, 345
Lites B.W., Rutten R.J., Berger T.E., 1999, ApJ 517, 1013
Martínez-Pillet V., Lites B.W., Skumanich A.P., Elmore D.F., Seagraves P, 1994 In: Schuessler M., Schmitt W. (eds.), Solar Magnetic Fields, Cambridge University Press, p. 219
Nindos A., Zirin H., 1998, Solar Phys. 179, 253
Norton A.A., Ulrich R.K., Bush R.I., Tarbell T.D. 1999, ApJ 518, L123
Noyes R.W. 1967, Solar velocity fields. In: Thomas R.N.(ed.),Aerodynamic phenomena in Stellar Atmospheres, IAU Symp. 28, Academic Press, London, p. 293
Pallé P.L., Régulo C., Roca Cortés T., et al., 1999, A&A 341, 625
Rutten R. J., 1994, in M. Carlsson (ed.), *Chromospheric Dynamics*, Proceedings Miniworkshop, ITA, Oslo, 25
Rutten R.J., 2000, Challenges for the New Millennium. In: Garcia Lopez R.J., Rebolo R., Zapatero Osorio M.R. (eds.) 11th Cambridge Workshop on Cool Stars, Stellar Systems and the Sun, Astron. Soc. Pac. Conf. Series, (in press)

Rutten R. J., Uitenbroek H., 1991, Solar Phys. 134, 15
Scherrer P.H., Bogart R. S., Bush R. I. et al., 1995, Solar Phys. 162, 129
Schrijver C.J., Coté J., Zwaan C., Saar S.H., 1989, ApJ 337, 964
Schrijver C.J., Shine R., Hagenaar H., et al., 1996, ApJ 468, 921
Schrijver C.J., Title A.M., van Ballegooijen A.A., Hagenaar H.J., Shine R.A., 1997, ApJ 487, 424
Skumanich A., Smythe C., Frazier E.N., 1975, ApJ 200, 747
Solanki S.K., 1993, Space Sci. Rev. 63,1
Spruit H.C., 1997, Mem. Soc. Astron. Ital. 68, 397
Staiger J., Schmieder B., Deubner F.L. et al. 1984, Mem. Soc. Astron. Ital. 55, 147
Straus T., 1995, Ph. D. Thesis, University of Firenze, Italy
Topka K.P., Tarbell T.D., Title A.M., 1997, ApJ 484, 479
von Uexküll M., Kneer F., 1995, A&A 294, 252
Vernazza J.E., Avrett E.H., Loeser R., 1981, ApJS 45, 635
Ulrich R.K., 1996, ApJ 465, 436